Insights into the structure and stability of the carbonic acid dimer†

Juliana Murillo,[a] Jorge David[b] and Albeiro Restrepo*[c]

Received 23rd February 2010, Accepted 10th June 2010
DOI: 10.1039/c003520c

In this paper we report the geometries and properties of 40 structural isomers located on the MP2/6-311++G** PES of the carbonic acid dimer. All six possible combinations of carbonic acid monomers were considered. The dimers are divided into six geometrical motifs. Our data suggests that combinations of *anti–anti* monomers do not necessarily lead to larger stabilization energies in the formation of the dimers. MP2 underestimates the relative binding energies with respect to CCSD(T) by as much as 3.2 kcal mol^{-1}. At least 3 different dimers which may contribute to the stability of carbonic acid are predicted to have significant populations. Binding energy is only directly related to relative stability when comparing dimers formed from the same monomers. Overall stabilization is mainly dictated by attractive electrostatic interactions *via* cooperative polarization by virtue of the spatial arrangement of the dipole moment components along the polar bonds. Shorter O···H bond distances and larger bond orders predicted for the hydrogen bonds directed towards carbonyl groups make for stronger hydrogen bonding than in O···H bonds directed towards hydroxyl groups.

Introduction

Carbonic acid (H_2CO_3, CA) is a very important molecule, its chemistry has implications in a wide variety of transcendental processes, we cite a few relevant ones:

(i) CA is known to be an intermediate in the respiratory evacuation of CO_2; the carbonic anhydrase enzyme catalyzes the conversion of CO_2 into H_2CO_3 and its dissociation to produce HCO_3^-, which dissolves in blood plasma and is then transported to the lungs where the reaction is reversed releasing CO_2. The mechanism requires hydrogen bonding networks to lower proton transfer barriers.[1–3] The pH in mammalian blood is regulated by a H_2CO_3/HCO_3^- buffer. There is a large number of variations of carbonic anhydrase, some mutated forms are believed to be responsible for osteopetrosis and mental retardation.[1]

(ii) Large amounts of CO_2 emitted to the atmosphere from the combustion of fossil fuels have been absorbed by the oceans,[4] where carbonic acid is produced and dissociated by the $CO_2 + H_2O \leftrightarrow H_2CO_3 \leftrightarrow HCO_3^- + H^+$ series of reactions, resulting in net acidification of seawaters. Dore and coworkers[5] documented a long term decreasing trend of -0.0019 ± 0.0002 y^{-1} in surface water pH, the report is based on carefully taken data over 20 years in the Central North Pacific Ocean near Hawaii; the authors report daily changes of as much as 0.01 in the water pH. The same work reports that the mean pH of the surface global ocean has decreased from $\approx$8.2 to 8.1 since pre-industrial times; the results lead to the conclusion that about 38% of the 0.1 decrease in pH over the last 250 years happened during the 20 years the study took place. On the other hand, a study on the pH of the oceans over the last 60 million years,[6] reveals much more acidic ancient conditions (pH = 7.42, 60 million years ago) and fluctuations over the last 25 million years (minimum 8.04, maximum 8.31 in that span), with the previous value of 8.1, the current pH, happening around 85 000 years ago.

(iii) The CO_2 and H_2O needed to form carbonic acid have been detected in sufficient abundances in comets,[7] interstellar space,[8] and in the surfaces of planets (Mars)[9] and moons (Europa and Ganymede),[10] the radiation and environmental conditions needed for the reaction to happen[11] are also appropriate in those places; this raises the possibility of CA being a major player in outer space chemistry.[11,12] Zheng and Kaiser explicitly addressed this issue: "Our experimental results indicate that carbonic acid might be present in the solar system ices that contain both water and carbon dioxide and are exposed by radiation from the solar wind and planetary magnetospheres".[11] The earth's upper atmosphere is also a suitable environment for the presence of gaseous carbonic acid.[12]

Despite long standing skepticism about the existence of carbonic acid, experimental and theoretical evidence suggests that it is a stable discrete molecular species.[12–18] The Potential Energy Surface (PES) for internal rotation exhibits three stable conformers depicted in Fig. 1: *anti–anti* (aa), *anti–syn* (as) and *syn–syn* (ss). The aa conformer is the most stable, followed closely by the as (1.9 kcal mol^{-1} above aa) and more distantly by the ss (11.8 kcal mol^{-1} above aa).[19] CA can be formed by dissolution of CO_2 into water, however, only a few molecules of actual CA are present in the solution.[20] CA is thermodynamically unstable with respect to CO_2 and H_2O as it rapidly decomposes in aqueous environments *via* exothermic

[a] *Departamento de Ciencias Químicas, Facultad de Ecología y Recursos Naturales, Universidad Andrés Bello, Avenida República 275, Santiago, Chile*
[b] *Escuela de Ciencias y Humanidades, Departamento de Ciencias básicas, Universidad Eafit, AA 3300 Medellín, Colombia*
[c] *Grupo de Química-Física Teórica, Instituto de Química, Universidad de Antioquia, AA 1226 Medellín, Colombia. E-mail: albeiro@matematicas.udea.edu.co*

† Electronic supplementary information (ESI) available: Cartesian coordinates for all optimized geometries reported in this paper; calculated IR for the 5 structures of Group I. See DOI: 10.1039/c003520c

reaction; a 10.4 kcal mol^{-1} energy difference for the process was predicted at the QCISD(T)/6-311++G** level by Wight and Boldyrev.[19] It has been pointed out that it requires only three water molecules around CA to approach the experimental decomposition rate,[21] however, sophisticated calculations have shown that water-free H_2CO_3 is kinetically very stable with a half life of about 180 000 years at ambient temperature.[16] CA was first observed in 1987 in the decomposition products of $(NH_4)HCO_3$;[13] Moore and Khanna produced the first pure H_2CO_3 samples in 1991.[22] To our knowledge, there are two well established synthetic routes to produce carbonic acid: high energy irradiation of cryogenic CO_2/H_2O mixtures[22–29] and cryogenic protonation of carbonate or bicarbonate.[12,14,30–33] Two polymorphic forms of carbonic acid termed α,β-H_2CO_3 have been identified.[34] Hage and coworkers have shown that α-H_2CO_3 can be sublimated and recondensed without decomposition.[33]

The thermodynamic instability of CA towards decomposition into CO_2 and H_2O is compensated by the formation of very stable dimers as evidenced by CCSD(T)/6-311++g(3df, 2dp) computations, which afforded a gas phase dimerization energy of −16.9 kcal mol^{-1};[15] in addition, Tossell found that it is not possible to explain the IR spectra of H_2CO_3 using monomer conformations, while the dimer calculated spectrum is in much better agreement with experiment.[20] This has lead researchers to postulate that dimers and possibly higher order clusters may contribute to the stabilities of solid and gaseous CA.[12,15,20,34–37] CA clusters are stabilized by cooperative hydrogen bonding. Given the three possible conformations of CA, there are six possible monomer combinations resulting in dimers (aa + aa, aa + as, aa + ss, as + as, as + ss, ss + ss). CA dimers and clusters arising from combinations of the aa monomer may not be the only contributors to the stability. Parra and coworkers for example,[38] have shown that although the ss conformation is the least stable of the three minimum energy isomers of CA, its clusters benefit considerably from the cooperativity effects present in ring-like networks. In another example, Winkel *et al.*,[34] showed that the as conformer gave slightly lower lattice energies than the aa conformer, making polymorphs of either conformer feasible and leading to growth errors in attempts to crystallize ordered structures. The question of CA dimer structure and stability, whose study we undertake in this paper is very relevant in light of the preceding discussion.

A problematic issue in the study of molecular and atomic clusters is the generation of equilibrium structures. Recently,[39–41] a modification of the Metropolis acceptance test in the simulated annealing optimization procedure[42–44] was proposed as means of generating cluster candidate structures that undergo further optimizations by traditional gradient following techniques. The method, incorporated into the ASCEC (after its Spanish acronym Annealing Simulado Con Energía Cuántica) program,[41] retains the comparative advantages and disadvantages of stochastic optimization over analytical methods,[45] namely, initial guess independence, exhaustive exploration of the potential energy surface, and the ability to jump over energy barriers and to sample several energy wells on the same run without getting trapped in local minima; however, the method is still computationally intensive because of repetitive evaluation of the energy function. The method has been successfully applied to the studies of the water tetramer,[39] small neutral and charged lithium clusters,[40] and the methanol tetramer,[46] affording contributing new structures never before reported in the literature which have helped us rationalize the stabilization of hydrogen-bonded networks. This work tackles the issue of stability of all possible CA monomer combinations to produce stable dimers in an effort to help in the understanding of the structure and stability of carbonic acid.

Computational details

The $(H_2CO_3)_2$ PES was explored by calculating every possible combination of monomers into dimers (aa + aa, aa + as, aa + ss, as + as, as + ss, ss + ss). We used the molecular cluster capabilities of the ASCEC program which contains an adapted version of the Simulated Annealing optimization procedure. The annealing algorithm was used to generate candidate structures after random walks of the PM3[47,48] PES for all monomer combinations.

The hybrid B3LYP density functional[49–51] in conjunction with the 6-31+G* basis set was used to optimize and characterize the structures afforded by ASCEC; this choice of methodology has proven to give very good quality results at a reasonable computational cost in the study of small hydrogen bond networks.[46,52] Further refinement and characterization of the stationary points was carried out by using second order perturbation theory at the MP2/6-311++G** level. Analytical harmonic second derivative calculations were used to characterize all stationary points as true minima (no negative eigenvalues of the Hessian matrix) or saddle points. Highly correlated CCSD(T)[53] energies were calculated on all the MP2 located minima using the aug-cc-pvdz basis set. All calculations in this work used the frozen core approximation.

Binding energies (BE) were calculated by subtracting the energy of the dimer from the energy of the given monomers, in this way, larger positive numbers correspond to larger stabilization energies. Relative binding energies (ΔBE) were calculated as the difference between the energy of the most stable dimer and the energy of a particular structure. In a previous study on the CA dimer, Liedl *et al.*,[15] found that the zero-point energy correction (ZPE) converges very fast on increasing the level of theory and that it is only a very minor source of errors; we followed this observation by calculating the ZPE at the MP2 level over the geometry of the most stable dimer optimized with several basis sets. Our results agree with the conclusions of Liedl and coworkers[15] (see below), accordingly, we used the MP2/6-311++G** ZPE to correct the CCSD(T) electronic energies in the calculations of binding energies and relative stabilities. The same study suggests that counterpoise correction (CC) for basis set superposition error (BSSE) shows poor results for this particular problem, $(H_2CO_3)_2$, and for the related hydrogen bonded dimers $(HF)_2$[54,55] and $(H_2O)_2$.[56] In this work, we use CC for BSSE to study the structures of the most stable group (see below), and conclude that correcting for BSSE makes very little difference, therefore, we restrain ourselves from applying such methodology to the rest of the structures. All optimization, frequency, and energy

calculations were carried out using the Gaussian 03[57] suite of programs. Wiberg bond orders were calculated according to the NBO program as implemented in Gaussian.

Results and discussion

ASCEC conditions

We used the big bang approach to construct the initial geometries for all ASCEC runs, namely, the two carbonic acid molecules were placed at the same position, allowing them to evolve under the annealing conditions. All six monomer combinations were run twice each, changing only the initial temperature from run to run. The systems were placed inside cubes of 6 Å of length; the PM3 semiempirical Hamiltonian was used to calculate the energy of a Markovian chain of randomly generated dimer configurations; we used geometrical quenching routes with initial temperatures of 350 and 300 K, a constant temperature decrease of 5% and 100 total temperatures.

Cluster structures

The dimer equilibrium geometries were produced following the procedure outlined above. All geometry optimizations were carried out with no imposition of symmetry constraints as the structures coming from ASCEC are randomly generated and belong to the C_1 point group, however some of the located stationary points have higher symmetries.

Geometries. We found 40 equilibrium structures on the MP2/6-311++G** PES classified into six different geometrical motifs shown in approximate decreasing order of stability in Fig. 2–7. Fig. 8 shows the relative stability of the structures and groups. An energy overlap between motifs due to the many geometrical possibilities is observed, a similar behavior was previously reported for the $(CH_3OH)_4$ PES.[46] Our classification is arbitrary: some groups may be considered as distortions of more stable groups. We named the structures by two criteria, global relative stability (1, 2,...,40; 1 being the most stable) and relative stability within each group (I_a, I_b,...,VI_d; I_a being the most stable in group I, and so on). There are plenty of possibilities and probably more structures to be found within each group due to combinations of two types of hydrogen bonds and three kinds of constituting monomers. The interactions responsible for the stabilization of the dimers are not enough to cause significant changes in the geometries of the monomers, except for some cases involving the ss unit (see below). A remarkable finding is that despite having no chiral centers, due to the spatial orientation of the entire dimer, we identified several pairs of specular images; counting only one structure for each of the 11 enantiomer pairs, would reduce the number of distinct conformations for $(H_2CO_3)_2$ located here to 29.

Brief description of the groups. Group I contains the 5 most stable dimers; it is the most known and widely reported geometrical motif for CA dimers; there are two hydrogen bonds involving a total of 4 oxygen atoms; each constituting molecule acts simultaneously as donor and acceptor of hydrogen bonds; the three most stable structures have two C=O···H bonds while the other two have one C=O···H and one H–O···H bond; only the structures with both hydrogen bonds directed towards carbonyl groups are planar; in every case, there are two hydrogen atoms left out from the stabilizing hydrogen bonding network; this group contains combinations of aa and as monomers.

Group II is characterized by a smaller central motif containing two hydrogen bonds involving a total of three oxygen atoms; there are two sets of enantiomer pairs; the following are common features of the 11 structures of this group: one molecule acts as donor and acceptor of hydrogen bonds of the C=O···H, H–O···H types while the hydroxyl group of the second molecule acts simultaneously as donor and acceptor of such bonds; all atoms involved in the stabilizing network are coplanar; there are two hydrogen atoms not participating in the stabilizing network; the dimers have contributions form the aa, as and ss monomers.

Group III exhibits only one hydrogen bond oriented either towards a carbonyl or towards an hydroxyl group; we located 10 structures in this group divided into 5 sets of enantiomer pairs; all three monomers contribute to the dimers of group III.

The six structures of group IV, divided into three sets of enantiomer pairs, have the following common features: one of the constituting molecules in the ss conformation donates two hydrogen bonds which are accepted by an oxygen of either a carbonyl or hydroxyl group in the second molecule, which in turn always donates a hydrogen bond towards a hydroxyl group from the first molecule, the addition of the third hydrogen bond distorts the geometry of the ss monomer lifting one of the C–O bonds between 15–20 degrees above the plane of the original ss conformation; there are four oxygen atoms involved in the stabilizing network; one hydrogen atom does not participate in hydrogen bonding; all three monomers contribute to the dimers.

Group V contains four structures, the geometries of this group are different from the geometries of group IV only because of the absence of the third hydrogen bond; three oxygen atoms participate in the stabilizing planar network and two hydrogen atoms are left out from it; all three monomers are found on the dimers of group V.

Group VI features a geometrical arrangement reminiscent of the geometries of group I: there are only two hydrogen bonds with participation of four oxygen atoms and two hydrogen atoms from the same molecule, there are two inactive hydrogen atoms from the second molecule; all dimers here are composed by a distorted ss monomer interacting as double donor with a second molecule acting as double acceptor of the hydrogen bonds; four structures with 1 set of enantiomer pairs were located in this group.

C=O···H and H–O···H hydrogen bonds are responsible for bonding between the two monomers. In most cases, the defining motifs are nonplanar. There are many instances of oxygen atoms acting as double acceptors of hydrogen bonds. O···H distances in H–O···H bonds are predicted to be ≈ 7% larger on average than in C=O···H bonds; the smallest and largest O···H distances in a C=O···H bond are, respectively 1.65 and 2.12 Å (1.87 Å average, $r_{max} - r_{min} = 0.25$ Å), while for H–O···H bonds those distances are 1.80 and 2.40 Å (2.00 Å average, $r_{max} - r_{min} = 0.60$ Å). Plots of the distributions of

O···H distances for both types of hydrogen bonds are included in Fig. 9. Both distributions resemble Gaussian functions; the wider range for H–O···H bonds makes for a large variety of possibilities, contributing to a rich conformational space.

The rich PES obtained in this study (40 structures, 6 geometrical motifs) is a consequence of the stochastic nature of the search of the quantum conformational space performed by the ASCEC program, which bypasses the structure-guessing step in the search for local minima.[39,40] The combinations of two types of hydrogen bonds and three types of monomers to make up the dimers, act in conjunction to increase the conformational possibilities; a similar effect was observed in the exploration of the $(CH_3OH)_4$ PES;[46] in contrast, water tetramers held together exclusively by one type of hydrogen bond and formed from only one type of monomer exhibit three geometrical motifs and eight structures.[39]

Energies, cluster stabilization and other properties. Table 1 classifies the structures in decreasing order of stability as predicted by CCSD(T)/aug-cc-pvdz//MP2/6-311++G** calculations; Table 1 also shows relative energies (ΔE), binding energies (BE) and relative binding energies (ΔBE) at the CCSD(T) and MP2 levels and information about the constituting monomers. Notice the stability overlap between groups already pointed out and shown in Fig. 8.

Very interesting observations are drawn from Table 1: binding energy is only directly related to relative stability when comparing dimers formed from the same monomers, however, when two dimers have different constituent moieties, there is an apparent conflict in the information provided; for example, dimers 2 and 3 have CCSD(T) total energies that are 0.7 and 1.3 kcal mol^{-1} above dimer number 1, the most stable structure, however, dimer 3 has the largest binding energy among all 40 dimers; dimers 1 and 2 show smaller binding energies than dimer 3 by 1.6 and 0.9 kcal mol^{-1}, respectively. The puzzle is solved by identifying the components for each dimer: aa + aa, aa + as, as + as, for dimers 1, 2 and 3, respectively. Since the aa monomer is 1.9 kcal mol^{-1} more stable than the as unit,[19] the initial components for dimers 2 and 3 are about 1.9 and 3.8 kcal mol^{-1} above the components for dimer 1, therefore, going down to the level of the aa + aa dimer would require additional stabilization energy to compensate for the 1.9 and 3.8 kcal mol^{-1} initial energy differences. In any case, it is clearly seen from this particular example that combinations of aa monomers do not necessarily lead to larger stabilization energies in the formation of the dimers; this observation is in very good agreement with the findings of Winkel *et al.*,[34] who reported lower lattice energies for extended arrays of the as monomer than for arrays of the aa monomer. A general trend is that MP2 underestimates the relative binding energies with respect to CCSD(T) by as much as 3.2 kcal mol^{-1}, showing the need for high levels of correlation for accurate description of the energetics of the CA dimer. A Boltzmann distribution analysis calculated with the MP2 Gibbs free energies reveals at least 3 different dimers, 1, 2, and 3, with significant populations of $\approx$83, 14, and 3%, respectively.

Table 1 Energetic analysis for $(H_2CO_3)_2$: ΔE: Relative energy with respect to structure 1. BE: Binding energy. ΔBE: Relative binding energy with respect to structure 3. All CCSD(T)/aug-cc-pvdz calculations using the MP2/6-311++G** optimized geometries. All energies corrected with the MP2/6-311++G** ZPEs. All energies in kcal mol^{-1}. Enantiomer pairs are described in the same line

Structure	Combination	ΔE CCSD(T)	ΔE MP2	BE CCSD(T)	BE MP2	ΔBE CCSD(T)	ΔBE MP2
1, I_a	aa + aa	0.0	0.0	17.4	15.3	1.6	1.5
2, I_b	aa + as	0.7	1.0	18.1	16.0	0.9	0.9
3, I_c	as + as	1.3	1.8	19.0	16.9	0.0	0.0
4, I_d	aa + as	7.0	6.2	11.9	10.9	7.1	6.0
5, I_e	as + as	8.1	7.6	12.1	11.1	6.8	5.8
6, II_a	aa + aa	8.7	7.4	8.7	8.0	10.3	8.9
7,8, $III_{a,b}$	aa + as	9.1	8.6	9.7	8.4	9.3	8.4
9, II_b	aa + as	9.6	8.6	9.2	8.4	9.8	8.4
10,11, $III_{c,d}$	as + as	9.8	9.5	10.4	9.2	8.5	7.6
12, II_c	aa + as	9.9	8.7	8.9	8.3	10.0	8.6
13, II_d	as + as	10.7	9.8	9.6	8.9	9.4	8.0
14,15, $III_{e,f}$	aa + aa	10.9	9.2	6.5	6.1	12.5	10.7
16,17, $II_{e,f}$	as + as	12.3	11.9	7.9	6.8	11.0	10.1
18,19, $III_{g,h}$	as + as	12.4	11.5	7.9	7.2	11.1	9.6
20, II_g	aa + as	13.0	11.0	5.9	6.0	13.1	10.9
21,22, $II_{h,i}$	as + as	14.3	12.5	5.9	6.2	13.0	10.7
23,24, $IV_{a,b}$	aa + ss	14.5	15.1	12.3	11.4	6.7	5.4
25, II_j	as + as	15.3	14.0	5.0	4.7	14.0	12.1
26,27, $IV_{c,d}$	as + ss	15.3	16.1	12.9	12.1	6.1	4.8
28, V_a	as + ss	16.8	17.1	11.4	11.2	7.6	5.7
29, VI_a	as + ss	17.6	17.6	10.6	10.6	8.4	6.2
30,31, $VI_{b,c}$	aa + ss	18.6	17.5	8.2	9.0	10.8	7.9
32, V_b	as + ss	19.2	18.1	7.6	8.5	11.4	8.4
33,34, $III_{i,j}$	as + ss	20.5	20.8	7.7	7.4	11.3	9.4
35,36, $IV_{e,f}$	as + ss	21.1	20.8	7.2	7.4	11.8	9.4
37, V_c	as + ss	21.1	20.1	7.1	8.2	11.9	8.7
38, II_k	as + ss	22.1	21.6	6.1	6.7	12.9	10.2
39, V_d	ss + ss	24.6	25.9	11.6	11.8	7.4	5.0
40, VI_d	ss + ss	25.6	27.0	10.6	10.8	8.4	6.1

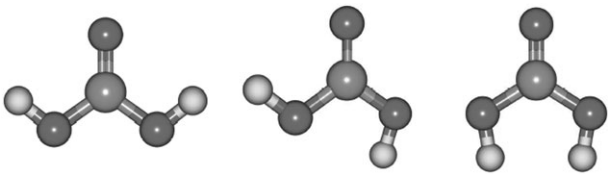

Fig. 1 Rotational conformers of carbonic acid. From left to right: *anti–anti* (aa), *anti–syn* (as, 1.9 kcal mol^{-1} above aa)[19] and *syn–syn* (ss, 11.8 kcal mol^{-1} above aa).[19] All conformations are planar.

We investigated the effect of the size of the basis set on the calculated ZPE. As a test case, we used the most stable dimer, structure 1 (Fig. 2). We reoptimized the structure at the MP2 level with several basis sets in an effort to account for the effects of larger divisions of the valence shells and for the inclusion or not of polarization and diffuse functions. Our calculations afforded the results listed on Table 2. The calculated ZPEs clearly justify our choice of MP2/6-311++G** ZPE to correct for the CCSD(T) energies because all calculated values are very close to 51.5 kcal mol^{-1}.

The counterpoise correction for BSSE was also tested in the five structures of Group I. We calculated the total BSSE corrected energy for the five configurations at the CCSD(T)/aug-cc-pvdz//MP2/6-311++G** level and obtained the results shown in Fig. 10. A very good linear correlation is observed ($y = 0.97x + 0.26$, $R^2 = 0.998$), which shows that BSSE only increases the ΔE by a small amount. A similar analysis was performed by reoptimizing the geometries at the MP2/6-311++G** lelvel accounting for the BSSE during the optimization; an equivalent trend for the MP2 BSSE corrected energies was observed ($y = 0.95x + 0.27$, $R^2 = 0.997$). This results validate our choice of not applying the CC for BSSE to the remaining structures as it clearly does not change the observed tendencies nor the magnitudes of the energy differences between dimers.

Combining the observations from Table 1 and from Fig. 2–7, we rationalize the stabilizing effects as follows: overall stabilization is mainly dictated by attractive electrostatic interactions *via* cooperative polarization by virtue of the spatial arrangement of the dipole moment components along the polar bonds which produce favorable molecular geometries. In this way, the structures of group I exhibit planar (structures 1, 2, 3, Fig. 2) and non-planar (structures 4, 5, Fig. 2) octapole-like configurations (or equivalently double quadrupoles or

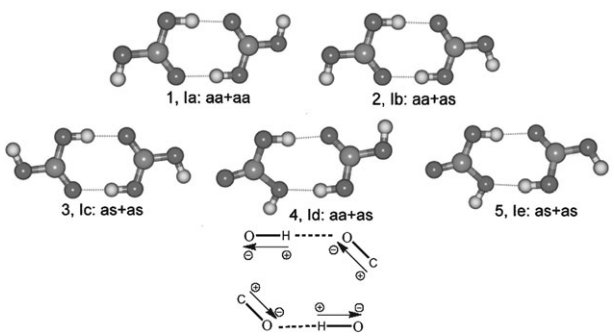

Fig. 2 Group I. Structures 1, 2 and 3 are planar, structures 4 and 5 are not. The network of stabilizing electrostatic interactions is shown.

Table 2 MP2 calculated ZPE (kcal mol^{-1}) as a function of the quaility of the basis set for dimer 1

Basis set	ZPE
6-31G*	51.7
6-31+G*	51.2
6-31+G**	51.5
6-311+G*	51.3
6-311+G**	51.5
6-311++G**	51.5

quadruple dipoles) with the individual dipole components arranged to maximize the attracting electrostatic interactions; the structures of group II (Fig. 3) show a planar arrangement of only three dipole components, which is not as stabilizing as the four interactions of group I; the configuration of the dipole components for the remaining groups decrease their stabilizing power due to less favorable orientations as we advance in the groups. A similar effect has already been observed in the study of the water[39] and methanol tetramers.[46] The overlap between groups is due to other kinds of stabilizing/destabilizing interactions, like favorable/unfavorable orientations of the remaining of the molecules, *etc*. Within-group stabilization is mostly due to the types of participating hydrogen bonds, and to the nature of the constituting monomers. For example, among the dimers of group I, structures 1, 2 and 3, are the most stable because of the presence of two hydrogen bonds directed towards carbonyl groups, while in structures 4 and 5, one of the hydrogen bonds is directed towards the hydroxyl group, resulting in a reduced stability and lack of planarity because of the out of plane orientation of the lone-pairs available to accept hydrogen bonds in the hydroxyl group. The relative stability of structures 1, 2 and 3, having the same hydrogen bonding network is then determined by the constituting monomers: aa + aa *vs.* aa + as *vs.* as + as, respectively. We tested this hypothesis by calculating the total electrostatic energy arising from contributions of all Mulliken predicted atom charges belonging to the stabilizing hydrogen bond network.[58] A plot of total electrostatic energy for the interactions of all point charges at the positions of the atoms belonging to dipole components along the hydrogen bonds against binding energies for all the structures in group I is depicted in Fig. 11. We point out a trend of larger dimer stabilization energies for larger (more negative) electrostatic contributions.

Our calculations lead to an interesting conclusion regarding comparative strengths of C=O···H and H–O···H hydrogen bonds. We pointed out above that the average O···H distance is ≈7% smaller when the hydrogen bond is directed towards a carbonyl group; furthermore, an analysis of the Wiberg bond orders afforded 0.0552 and 0.0656 for the hydrogen bonds in C=O···H for structures 4 and 5, respectively, and 0.0354 and 0.0485 for the H–O···H hydrogen bonds in the same structures; notice that between isomers 4 and 5, 4 being the most stable shows smaller bond orders for the hydrogen bonds; the apparent conflict was resolved earlier by realizing that dimer 5, although less stable than dimer 4, is predicted to have a larger interaction energy because of its particular monomer combination (Table 1). We conclude that shorter

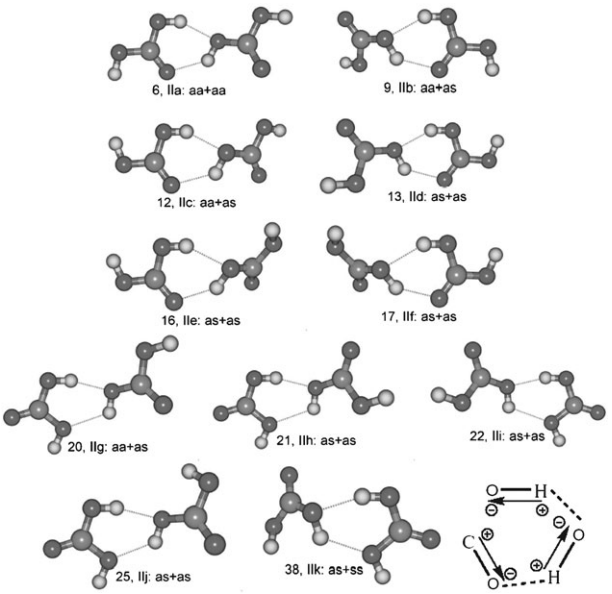

Fig. 3 Group II. Structures (16, 17) and (21, 22) are enantiomer pairs. The network of stabilizing electrostatic interactions is shown.

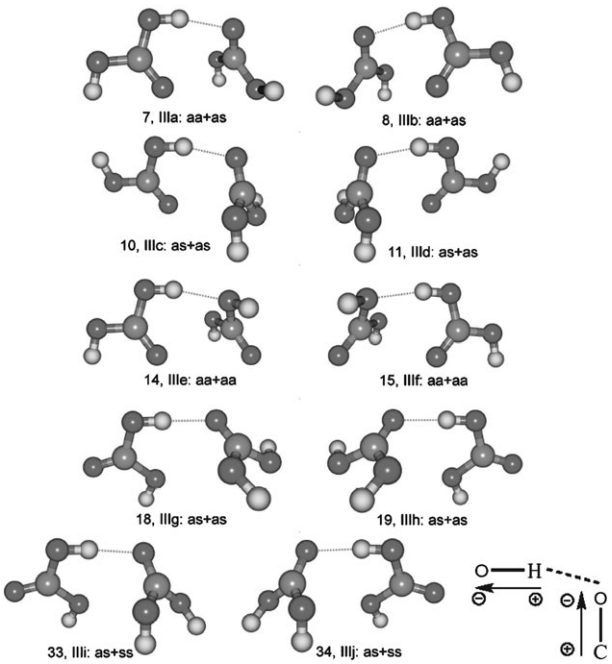

Fig. 4 Group III. Structures (7, 8), (10, 11), (14, 15), (18, 19), (33, 34) are enantiomer pairs. The network of stabilizing electrostatic interactions is shown.

bond distances and larger bond orders predicted for the C═O···H make for stronger hydrogen bonding than in H–O···H. Many details of hydrogen bonding remain unclear,[59] probably due in part to the difficulties in accurate theoretical treatment of the complex energy decomposition schemes for these interactions,[60] thus, there are probably other aspects to be touched upon in the previous discussions, nonetheless our explanations seem to be plausible steps in the goal of unraveling the intricacies of the structure and stability of the dimers of carbonic acid.

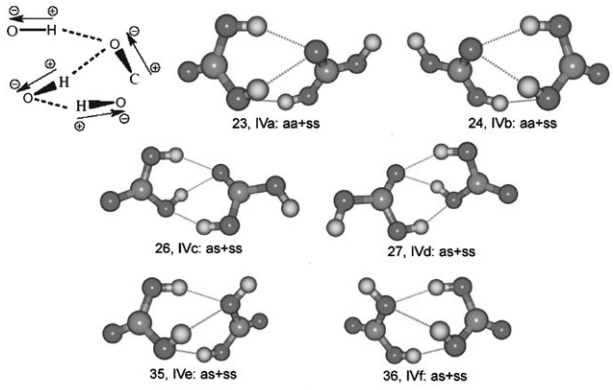

Fig. 5 Group IV. Structures (23, 24), (26, 27), (35, 36) are enantiomer pairs. The network of stabilizing electrostatic interactions is shown.

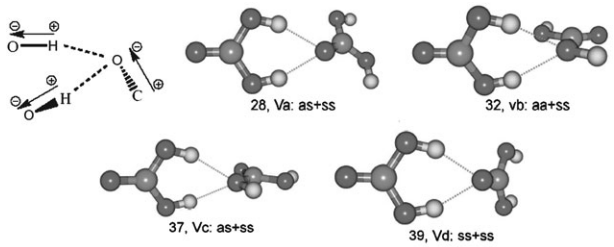

Fig. 6 Group V. The network of stabilizing electrostatic interactions is shown. All dimers have at least one ss monomer.

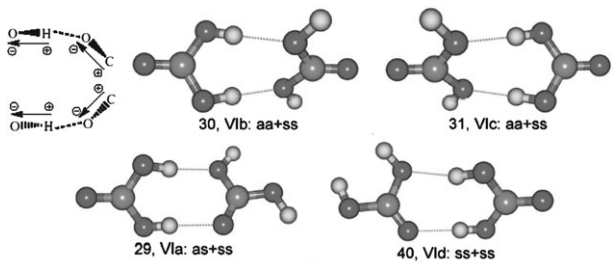

Fig. 7 Group VI. Structures (30, 31) are enantiomer pairs. The network of stabilizing electrostatic interactions is shown. All dimers have at least one ss monomer.

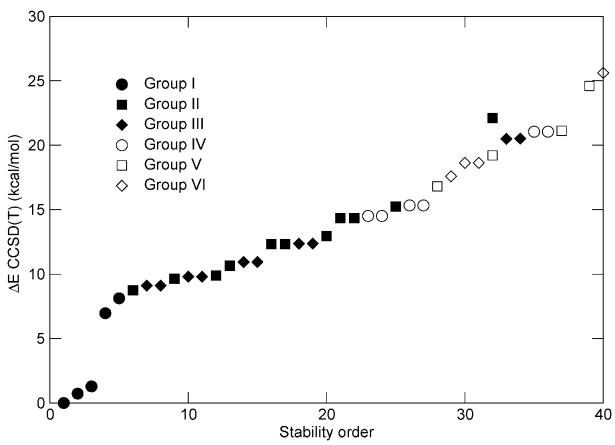

Fig. 8 Relative stabilities of the structural motifs for $(H_2CO_3)_2$. An overlap between groups is observed.

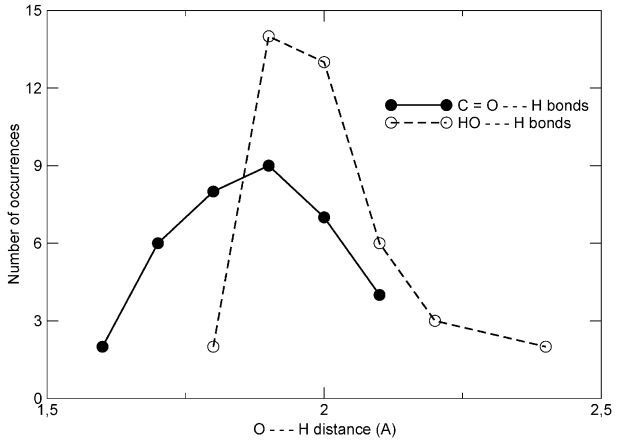

Fig. 9 Distribution of the O···H distances for C═O···H and HO···H hydrogen bonds in the carbonic acid dimer.

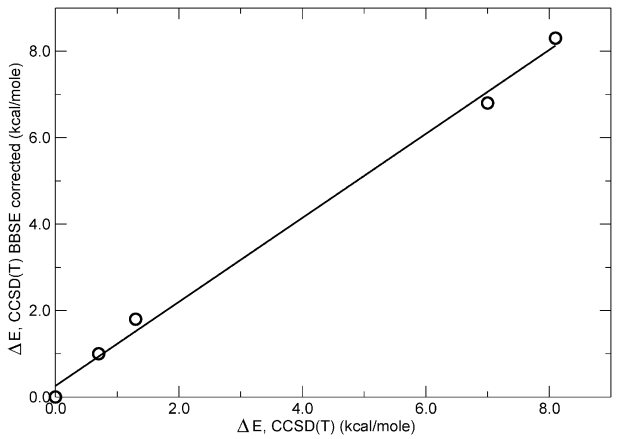

Fig. 10 BSSE on the CCSD(T)/aug-cc-pvdz relative energies calculated for the five structures of group I.

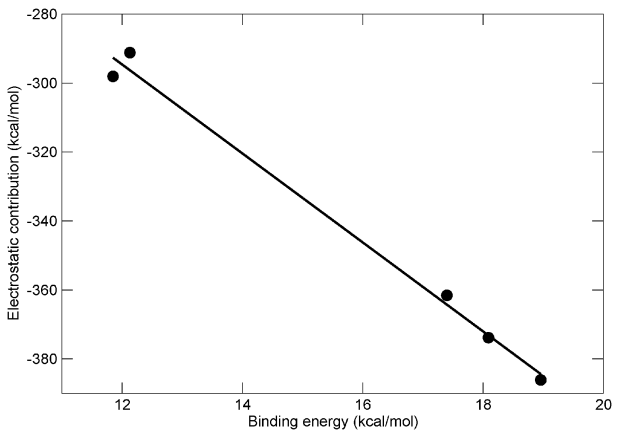

Fig. 11 Total electrostatic energy for the interactions of all point charges at the positions of the atoms belonging to dipole components along the hydrogen bond network for the structures of group I.[58]

Conclusions and perspectives

We report the geometries and properties of 40 structural isomers located on the MP2/6-311++G** PES of the carbonic acid dimer. The structures were found after random walks of the PM3 PES for all six possible combinations of carbonic acid monomers to produce stable dimers. The isomers are divided among six geometrical motifs. Despite having no chiral centers, we located 11 enantiomer pairs. Our data suggests that combinations of aa monomers do not necessarily lead to larger stabilization energies in the formation of the dimers, therefore, an accurate description of the carbonic acid dimer requires all possible combinations of monomers. MP2 underestimates the relative binding energies with respect to CCSD(T) by as much as 3.2 kcal mol^{-1}, showing the need for high levels of correlation for accurate description of the energetics of the CA dimer. A Boltzmann distribution analysis reveals at least 3 different dimers, 1, 2, and 3, with significant populations of ≈83, 14, and 3%, respectively. Binding energy is only directly related to relative stability when comparing dimers formed from the same monomers. Overall stabilization is mainly dictated by attractive electrostatic interactions *via* cooperative polarization by virtue of the spatial arrangement of the dipole moment components along the polar bonds. Stabilization within each group is mostly due to the types of participating hydrogen bonds and to the nature of the constituting monomers. Shorter bond distances and larger bond orders predicted for the C═O···H make for stronger hydrogen bonding than in H–O···H. The results in this study are by no means conclusive for a complete characterization of the CA_2 PES as there are probably more structures to be located due to the many conformational possibilities afforded by two possible hydrogen bond types and three possible monomeric units in this particular problem which lead to a rich conformational space.

Acknowledgements

Partial funding for this work by Universidad EAFIT, internal project number 173-000013 is acknowledged. We are thankful to the Instituto de Química, Universidad de Antioquia, for ample provisions of computer time. We thank professor Cacier Hadad, Universidad de Antioquia, for very helpful discussions about this work. We are thankful to professor Daniel Jaramillo, Universidad de Antioquia, for discussing with us the electrostatic interactions in this work. Professor Roald Hoffmann, Cornell University, gave us very useful suggestions, his help is greatly appreciated.

References

1 J. Berg, J. Tymoczko and L. Stryer, *Biochemistry*, W. H. Freeman and company, New York, 5th edn, 2002.
2 S. Fisher, C. maupin, M. Budayova-Spano, L. Govindasamy, C. Tu, M. Agbandje-Mckenna, D. Silverman, G. Voth and R. McKenna, *Biochemistry*, 2007, **46**, 2930.
3 S. Thoms, *J. Theor. Biol.*, 2002, **215**, 399.
4 C. Sabine, *et al.*, *Science*, 2004, **305**, 367.
5 J. Dore, R. Lukas, W. Sadler, M. Church and D. Karl, *Proc. Natl. Acad. Sci. U. S. A.*, 2009, **106**, 12235.
6 P. Pearson and M. Palmer, *Nature*, 2000, **406**, 695.
7 S. Kim, Y. Minh, S. Hyung, Y. Kim, E. van Dishoeck and F. van der Tak, *High Resolution Optical and Infrared Observations of Molecules in Comets: Chemistry in the Envelopes around Massive Young Stars, from Molecular Clouds to Planetary*, 2000, p. 471.
8 P. W. Ehrenfreund and W. Schutte, *Infrared Observations of Interstellar Ices, from Molecular Clouds to Planetary*, 2000, p. 135.
9 J. Longhi, *J. Geophys. Res.*, 2006, **111**, E06011.

10 N. Mason, *et al.*, *VUV Spectroscopy of Extraterrestrial Ices, Astrochemistry—from Laboratory Studies to Astronomical Observations*, 2006, p. 128–139.
11 W. Zheng and R. Kaiser, *Chem. Phys. Lett.*, 2007, **450**, 55.
12 W. Hage, K. Liedl, A. Hallbrucker and E. Mayer, *Science*, 1998, **279**, 1332.
13 J. Terlouw, C. Lebrilla and H. Schwarz, *Angew. Chem., Int. Ed. Engl.*, 1987, **26**, 354.
14 W. Hage, A. Hallbrucker and E. Mayer, *J. Am. Chem. Soc.*, 1993, **115**, 8427.
15 K. Liedl, S. Sekušak and E. Mayer, *J. Am. Chem. Soc.*, 1997, **119**, 3782.
16 T. Loerting, C. Tautermann, R. Kroemer, I. Kohl, A. Hallbrucker, E. Mayer and K. Liedl, *Angew. Chem., Int. Ed.*, 2000, **39**, 891.
17 H. Al-Hosney and V. Grassian, *J. Am. Chem. Soc.*, 2004, **126**, 8068.
18 H. Al-Hosney and V. Grassian, *Phys. Chem. Chem. Phys.*, 2005, **7**, 1266.
19 C. Wight and A. Boldyrev, *J. Phys. Chem.*, 1995, **99**, 12125.
20 J. Tossell, *Inorg. Chem.*, 2006, **45**, 5961.
21 C. Tautermann, A. Voegele, T. Loerting, I. Kohl, A. Hallbucker, E. Mayer and K. Liedl, *Angew. Chem., Int. Ed.*, 2002, **8**, 66.
22 M. Moore and R. Khanna, *Spectrochim. Acta, Part A*, 1991, **47A**, 255.
23 M. Moore, P. Khanna and B. Donn, *J. Geophys. Res.*, 1991, **96**, 17541.
24 N. Dellorusso, P. Khanna and M. Moore, *J. Geophys. Res.*, 1993, **98**, 5505.
25 J. Brucato, M. Palumbo and G. Strazzulla, *Icarus*, 1997, **125**, 135.
26 P. Gerakines, M. Moore and R. Hudson, *Astron. Astrophys.*, 2000, **357**, 793.
27 G. Strazzulla, G. Baratta, M. Palumbo and M. Sartore, *Nucl. Instrum. Methods Phys. Res., Sect. B*, 2000, **166–167**, 13.
28 M. Moore, R. Hudson and P. Geranikes, *Spectrochim. Acta, Part A*, 2001, **57**, 843.
29 C. Wu, D. Judge, B. Cheng, T. Yih, C. Lee and W. Ip, *J. Geophys. Res.*, 2003, **108**, 5032.
30 W. Hage, A. Hallbrucker and E. Mayer, *J. Chem. Soc., Faraday Trans.*, 1995, **91**, 2823.
31 W. Hage, A. Hallbrucker and E. Mayer, *J. Chem. Soc., Faraday Trans.*, 1996, **92**, 3183.
32 W. Hage, A. Hallbrucker and E. Mayer, *J. Chem. Soc., Faraday Trans.*, 1996, **92**, 3197.
33 W. Hage, A. Hallbrucker and E. Mayer, *J. Mol. Struct.*, 1997, **408–409**, 527.
34 K. Winkel, W. Hage, T. Loerting, S. Price and E. Mayer, *J. Am. Chem. Soc.*, 2007, **129**, 13863.
35 P. Ballone, B. Montanari and R. Jones, *J. Chem. Phys.*, 2000, **112**(15), 6571.
36 M. Nguyen, M. Matus, V. Jackson, V. Ngan, J. Rustad and D. Dixon, *J. Phys. Chem. A*, 2008, **112**, 10386.
37 J. Tossell, *Environ. Sci. Technol.*, 2009, **43**, 2575.
38 R. Parra, S. Bulusu and X. Zeng, *J. Chem. Phys.*, 2005, **122**(18), 184325.
39 J. Pérez, C. Hadad and A. Restrepo, *Int. J. Quantum Chem.*, 2008, **108**, 1653.
40 J. Pérez, E. Flórez, C. Hadad, P. Fuentealba and A. Restrepo, *J. Phys. Chem. A*, 2008, **112**, 5749.
41 J. Pérez and A. Restrepo, *ASCEC V-02: Annealing Simulado con Energía Cuántica*, Property, development and implementation: Grupo de Química–Física Teórica, Instituto de Química, Universidad de Antioquia, Medellín, Colombia, 2008.
42 N. Metropolis, A. Rosenbluth, M. Rosenbluth, A. Teller and E. Teller, *J. Chem. Phys.*, 1953, **21**, 1087.
43 S. Kirkpatrick, C. Gellat and M. Vecchi, *Science*, 1983, **220**, 671.
44 E. Aarts and H. Laarhoven, *Simulated Annealing: Theory and Applications; Springer*, New York, 1987.
45 A. Restrepo, F. Mari, C. Gonzalez and M. Marquez, *Quím., Actualidad Futuro*, 1995, **5**, 101.
46 J. David, D. Guerra and A. Restrepo, *J. Phys. Chem. A*, 2009, **113**, 10167.
47 J. Stewart, *J. Comput. Chem.*, 1989, **10**, 209.
48 J. Stewart, *J. Comput. Chem.*, 1989, **10**, 221.
49 P. Stephens, J. Devlin, C. Chabalowski and M. Frisch, *J. Phys. Chem.*, 1994, **98**, 11623.
50 C. Lee, W. Yang and R. Parr, *Phys. Rev. B: Condens. Matter*, 1988, **37**, 785.
51 A. Becke, *J. Chem. Phys.*, 1993, **98**, 5648.
52 S. Mejía, J. Espinal, A. Restrepo and F. Mondragón, *J. Phys. Chem. A*, 2007, **111**, 8250.
53 J. Pople, M. Head-Gordon and K. Raghavachari, *J. Chem. Phys.*, 1987, **87**, 5968.
54 K. Peterson and T. Dunning, *J. Chem. Phys.*, 1995, **102**, 2032.
55 S. Xantheas, *J. Chem. Phys.*, 1996, **104**, 8821.
56 M. Feyereisen and D. Dixon, *J. Phys. Chem.*, 1996, **100**, 2993.
57 M. J. Frisch, G. W. Trucks, H. B. Schlegel, G. E. Scuseria, M. A. Robb, J. R. Cheeseman, J. A. Montgomery, Jr., T. Vreven, K. N. Kudin, J. C. Burant, J. M. Millam, S. S. Iyengar, J. Tomasi, V. Barone, B. Mennucci, M. Cossi, G. Scalmani, N. Rega, G. A. Petersson, H. Nakatsuji, M. Hada, M. Ehara, K. Toyota, R. Fukuda, J. Hasegawa, M. Ishida, T. Nakajima, Y. Honda, O. Kitao, H. Nakai, M. Klene, X. Li, J. E. Knox, H. P. Hratchian, J. B. Cross, V. Bakken, C. Adamo, J. Jaramillo, R. Gomperts, R. E. Stratmann, O. Yazyev, A. J. Austin, R. Cammi, C. Pomelli, J. Ochterski, P. Y. Ayala, K. Morokuma, G. A. Voth, P. Salvador, J. J. Dannenberg, V. G. Zakrzewski, S. Dapprich, A. D. Daniels, M. C. Strain, O. Farkas, D. K. Malick, A. D. Rabuck, K. Raghavachari, J. B. Foresman, J. V. Ortiz, Q. Cui, A. G. Baboul, S. Clifford, J. Cioslowski, B. B. Stefanov, G. Liu, A. Liashenko, P. Piskorz, I. Komaromi, R. L. Martin, D. J. Fox, T. Keith, M. A. Al-Laham, C. Y. Peng, A. Nanayakkara, M. Challacombe, P. M. W. Gill, B. G. Johnson, W. Chen, M. W. Wong, C. Gonzalez and J. A. Pople, *GAUSSIAN 03 (Revision E.01)*, Gaussian, Inc., Wallingford, CT, 2004.
58 Dipole–dipole interaction energies are calculated within the multipole expansion by $[\mathbf{p}_1\cdot\mathbf{p}_2 - 3(\mathbf{n}\cdot\mathbf{p}_1)(\mathbf{n}\cdot\mathbf{p}_2)]/4\pi\varepsilon_0|\mathbf{x}_1 - \mathbf{x}_2|^3$ (see Jackson's book[61] for description of the symbols). The multipole expansion requires conditions not met in our case, namely ideal dipoles and that the distances between individual dipoles must be very large compared to the distance separating the charges of individual dipoles; therefore, as an indirect measure of the dipole–dipole interactions, we calculated the total electrostatic energy for the interactions of all point charges at the positions of the atoms belonging to dipole components along the hydrogen bond network.
59 M. Masella, N. Gresh and J. Flament, *J. Chem. Soc.*, 1998, **94**, 2745.
60 W. Koch and M. Holthausen, *Hydrogen Bonds and Weakly Bound Systems*, in *A Chemist's Guide to Density Functional Theory*, Wiley, New York, 2nd edn, 2002.
61 J. Jackson, *Classical Electrodynamics*, Wiley, New York, 3rd edn, 1998.

